Monograph:
Li, L.M. and Billings, S.A. (2009) Analysis of nonlinear oscillators in the frequency domain using volterra series Part II : identifying and modelling jump Phenomenon. Research Report. ACSE Research Report no. 989 . Automatic Control and Systems Engineering, University of Sheffield

Analysis of Nonlinear Oscillators in the Frequency Domain Using Volterra Series Part II : Identifying and Modelling Jump Phenomenon

L.M.Li and S.A.Billings

Department of Automatic Control
and Systems Engineering,
University of Sheffield, Sheffield
Post Box 600 S1 3JD
UK

Research Report No. 989

May 2009

Analysis of Nonlinear Oscillators in the Frequency Domain Using Volterra Series Part II : Identifying and Modelling Jump Phenomenon

L.M.Li and S.A.Billings∗

Department of Automatic Control and Systems Engineering

University of Sheffield

Sheffield S1 3JD

UK

∗S.Billings@sheffield.ac.uk

Abstract: In this the second part of the paper, a common and severe nonlinear phenomenon called jump, a behaviour associated with the Duffing oscillator and the multi-valued properties of the response solution, is investigated. The new frequency domain criterion of establishing the upper limits of the nonlinear oscillators, developed in Part I of this paper, is applied to predict the onset point of the jump, and the Volterra time and frequency domain analysis of this phenomenon are carried out based on graphical and numerical techniques.

1. Introduction

A new frequency domain criterion of finding the upper limits of a nonlinear oscillator with cubic stiffness was introduced in the Part I of this paper. A typical example of this kind of oscillator is the Duffing oscillator. The Duffing oscillator has been extensively applied to represent many practical systems and is often used as a benchmark example for nonlinear oscillator analysis. Summary works can be found in Hayashi(1964).

In this, Part II of this paper, a common severe nonlinear phenomenon, referred to as jump, induced by the multi-valued solution due to the cubic nonlinearity in the Duffing oscillator, is studied. Jump phenomenon is seemly a time domain phenomenon, but in fact it is closely associated with the Volterra/frequency domain representation, therefore the results from the first part of this paper are applied to explain the mechanism behind this phenomenon and to provide a prediction of the onset point for this behaviour change. In addition, time and frequency domain modelling of this phenomenon are performed.

2. Preliminaries

Consider the Duffing oscillator described as

$$m\ddot{y} + c\dot{y} + k_1 y + k_3 y^3 = u(t) \qquad \text{with } u(t) = A\cos(\omega t) \tag{1}$$

where m is the mass, c is the damping, k_1 and k_3 are the linear and cubic stiffness respectively, and the initial conditions are set equal to zero.

Despite the seemly simple form of Duffing's equation(1), it is extremely rich in dynamic behaviour and exhibits many complex solutions. Almost every nonlinear phenomenon can be found in Duffing's equation therefore it has often been used as a benchmark example in many studies. The bifurcation diagram in Figure 1 shows some typical dynamics of a Duffing oscillator with the parameters in (1) as

$$m = 1, c = 0.4, k_1 = 1, k_3 = 4 \tag{2}$$

at $\omega = 2.5$ rad/sec .

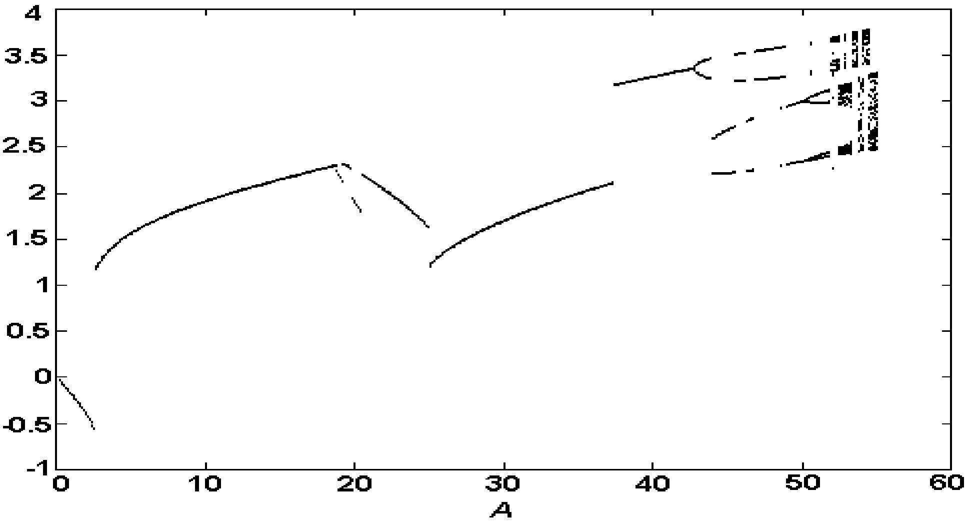

Figure 1. Bifurcation diagram for system (2)

It can be seen from Figure 1 that the Duffing oscillator experiences dramatic dynamic behaviours during the course of excitation amplitude changes. Among them, there is a period-doubling(1/2 subharmonics) for 43<*A*<50.5, a further period-doubling(1/4 subharmonics) for 50.5<*A*<52, leading to chaos regime for 52<*A*<55. Subharmonics and chaos are two of the most common phenomena occurring in nonlinear oscillators and have attracted constant interest and study over the past decades(Stoker, 1957; Nayfeh and Mook, 1979; Feigenbaum, 1980; Frey and Norman, 1992; Thompson and Stewart, 1991; Rao, 1995; Boaghe and Billings,2003; Li and Billings, 2005, etc).

Another commonly occurring nonlinear phenomenon is the shock jump, shown in Figure 1 over the excitation level $2 < A < 3$. As Pain(2005) pointed out the amplitude of the response is not single valued for a given frequency where shock jumps in response amplitude may occur.

A zoomed view is shown in Figure 2 for the amplitude of response against the excitation level around the jump, which is the main subject of this study. Unlike subharmonics and chaos, this kind of severe nonlinear problem has received little attention to date. In the following sections, the prediction, analysis and modelling of the jump phenomenon using Volterra series in the frequency domain are introduced for the first time.

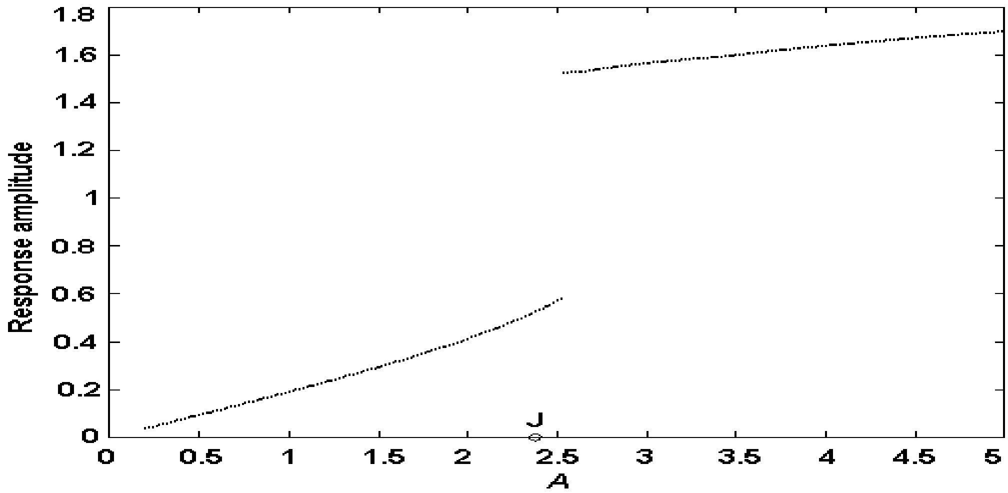

Figure 2. Response amplitude jump of system (2)

3. Analysis of jump phenomenon in the frequency domain

As noted in Section 2, the Duffing oscillator (1) can represent very complex dynamic behaviours. For such a driven nonlinear oscillator, closed-form analytical solutions are not available therefore approximation schemes are used in quantitative investigations. One of the approximation methods that have been widely adopted is the harmonic balance method. This involves re-arranging the external excitation in (1) as

$$u = P\sin(\omega t) + Q\cos(\omega t) \quad \text{with } A = \sqrt{P^2 + Q^2} \tag{3}$$

and expressing the response as

$$y = C\sin(\omega t) \tag{4}$$

Substituting (3) and (4) into (1), together with the use of $\sin^3(t) = \frac{3}{4}\sin(t) - \frac{1}{4}\sin(3t)$ yields

$$\tfrac{3}{4}k_3 H^3 \sin(\omega t) - mH\omega^2 \sin(\omega t) + cH\sin(\omega t) + k_1 H\omega c\cos(t) = P\sin(t) + Q\cos(t) \tag{5}$$

where the term containing $\sin(3\omega t)$ has been neglected.

Equating coefficients of the same harmonic terms in (5) and using $A = \sqrt{P^2 + Q^2}$ gives(Rao, 1995)

$$[\tfrac{3}{4}k_3 C^3 + (k_1 - m\omega^2)C]^2 + c^2\omega^2 C^2 = A^2 \tag{6}$$

Because of the cubic nonlinearity $k_3 \neq 0$, the response will be multi-valued, shown in Figure 3.

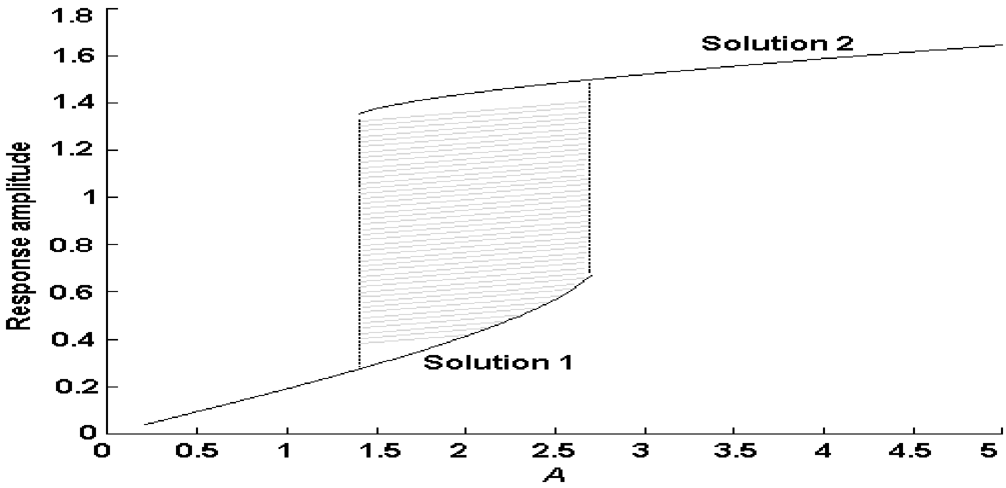

Figure 3. Harmonic Balance solutions from (6)

Comparing Figure 3 and Figure 2 reveals that the estimated harmonic balance solutions provide a good approximation of the real solution in terms of both value and trend. Inspection of Figure 3 reveals that, when increasing the amplitude *A* to around 1.4 until 2.8, two stable solutions will co-exist(the shadow range in Figure 3). When some certain conditions are met, the solution will jump from one to the other. However, (6) cannot provide any indication on why and when this type of severe dynamic change will happen.

It is easy to verify that for the Solution 1 range, the original system (2) can provide a valid Volterra series/GFRF representation for the underlying system. This also indicates that, considering the analytic nature of Volterra series representation, the original system (2) will no longer be valid in the Volterra/GFRF's domain from the start of Solution 2, or the response jumping point. This implies that the jumping point is the upper limit of the Volterra series representation for this type of nonlinear system. Recall that in the Part I of this paper a frequency domain criterion to obtain the upper limit of nonlinear oscillators with cubic stiffness subject to harmonic excitation was developed, rewritten here as (7)

$$\tilde{A}(\omega) = \frac{2}{\sqrt{|k_3|}(3|H_1(\omega)|)^{3/2}} \tag{7}$$

where $H_1(\omega)$ is the first order frequency response function.

The result of the new criterion (7) is shown in Figure 2 as point 'J', which is a good estimation of the real jump point. This is not exceptional but, as the following example shows, this is a general rule for this kind of problem.

Consider a Duffing oscillator with the parameters

$$m = 1, c = 0.2, k_1 = 1 \text{ and } k_3 = 0.05. \tag{8}$$

Figure (4) gives a clear overall picture of when and where the jump occurs along both varying excitation amplitude and frequency axes.

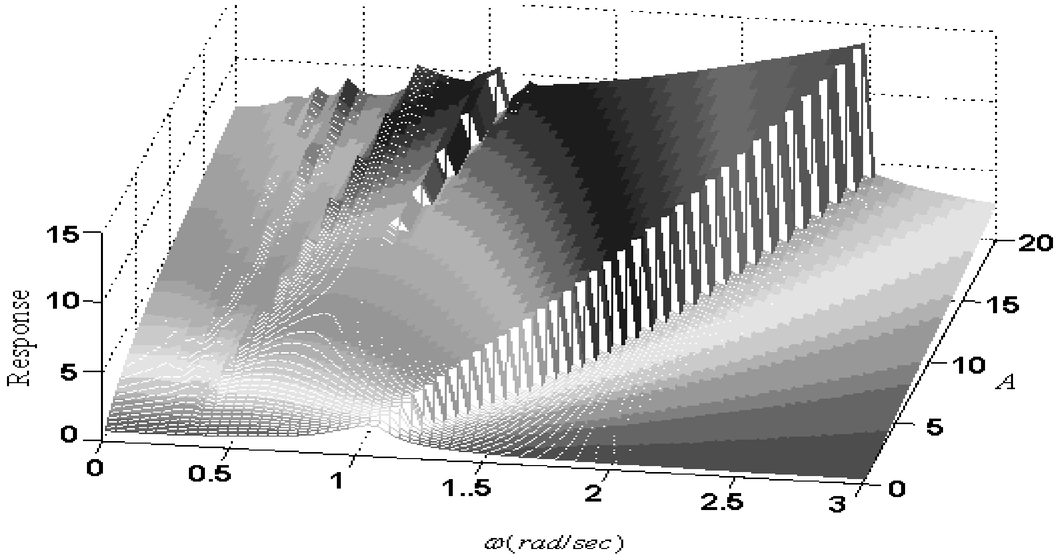

Figure 4. Response curve of the Duffing oscillator (8) for both varying excitation amplitude and frequency

The jump cliff starts from $\omega = 1$ *rad/sec* and A=1. The frequency point and the magnitude of the jump increase monotonically, as the amplitude of the excitation increases, showing a clear pattern. The rule that governs the pattern is indeed the criterion (7), as shown in Figure 5, in which the real jump line is the 2-D overhead view from Figure 4. It can be seen that the result by criterion (7) predicts very accurately the real jumping points.

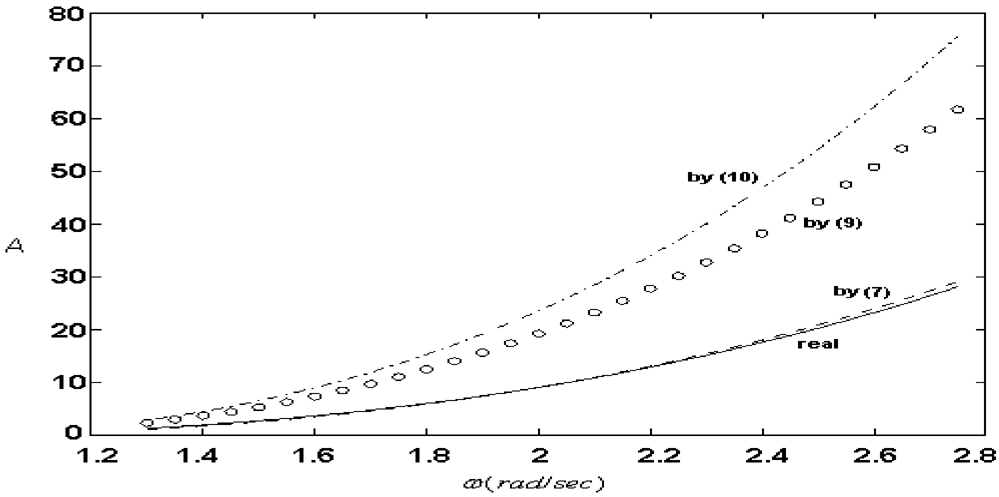

Figure 5. Comparison of real jump line with different Volterra criteria. Real—Solid; criterion (7)—Dashed; criterion (9)—circled, criterion (10)—dash dotted

For comparison, the recent frequency domain criteria by Tomlinson *et al*(1996) and Peng and Lang(2007) are also displayed in Figure 5, in which Tomlinson's criterion is defined as

$$\tilde{A}_T(\omega) < \left[\tfrac{2}{3}(k_3 \left|H_1(\omega)\right|^3\right]^{-\frac{1}{2}} \tag{9}$$

and Peng and Lang's criterion is defined as

$$\tilde{A}_P(\omega) < \frac{1}{|H_1(\omega)|\sqrt{\lambda k_3}} \tag{10}$$

where $\lambda = \max_{k=1,\ldots,\infty}\left(|H_1((2k-1)\omega|\right)$

Note that here the jumping line is the absolute splitting line dividing the validity and in-validity of the Volterra series representation for the original system. Clearly both (9) and (10) are significantly overestimated in the jumping case.

Take a cross section of Figure 4 at $\omega = 2$ rad/sec.

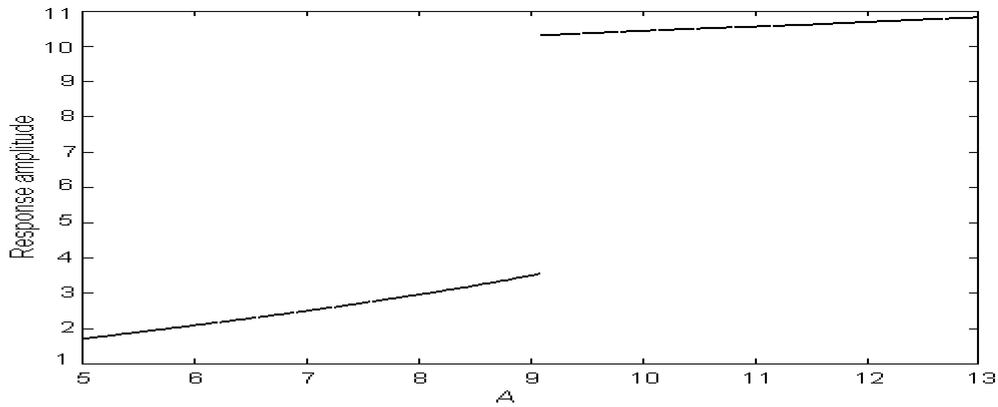

Figure 6. Response amplitude jump for system (8) at $\omega = 2$ rad/sec

In this example the jump occurs at *A*=9.09, which agrees very well with the criterion (7) at $\tilde{A}(\omega)\Big|_{\omega=2} = 9.06$. The new criterion (7) in the Part I of this paper was proposed based on the assumption that the system can be well described by the first few Volterra kernels and for which the higher order kernels fall off rapidly. This can be verified by exploring the response in terms of Volterra/GFRF representation right before and after the jump, as illustrated in Figure 7.

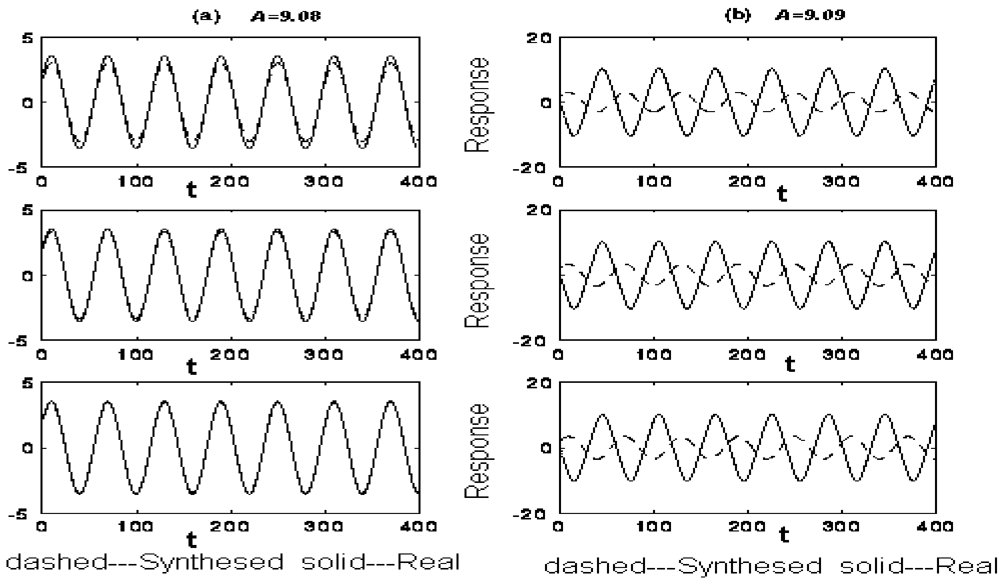

Figure 7. Comparison of real response and synthesized response by GFRF's before and after the jump. Top---First order response, middle -- up to the 3rd order response and bottom-- up to the 5th order response.

So far we can conclude that fast convergence or representation efficiency is likely to be the mechanism behind the triggering of jumping. When the amplitude of excitation increases to the upper limit of a fast convergence low order Volterra series representation as (7) suggested, the response will be forced to jump to the other stable solution routine, making the original Duffing system no longer valid in the Volterra/frequency domain. This dramatic dynamic change has its appearance in the time domain, but actually has solid roots in the frequency domain. It is of therefore of interest to make a frequency domain investigation using Response Spectrum Map(RSM) (Billings and Boaghe, 2001)

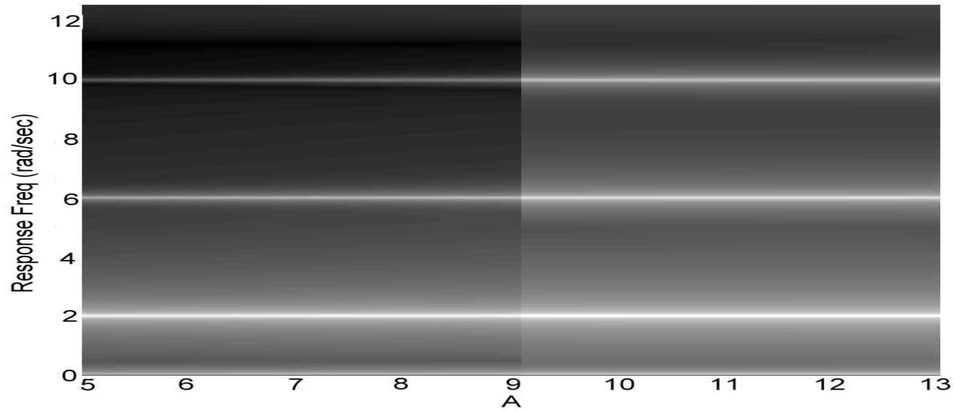

(a)

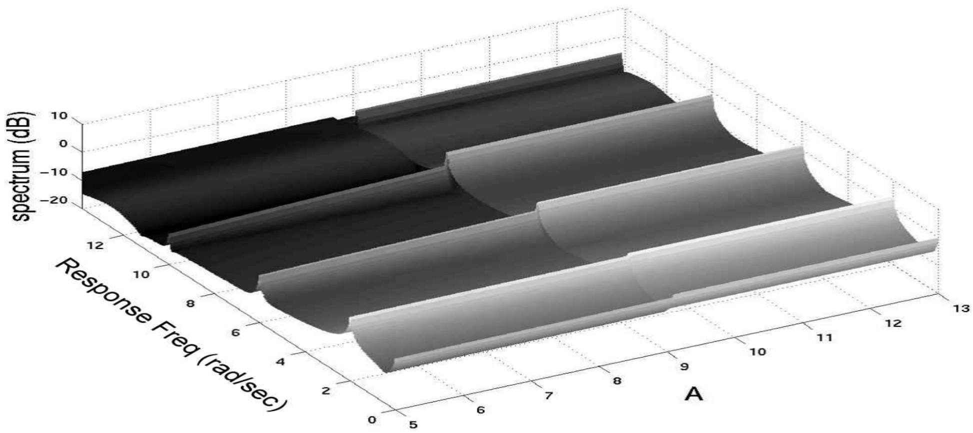

(b)

Figure 8. RSM for system (8) when the jump occurs; (a) 2D view and (b) 3D view

Figure 8 shows that the harmonic components of response remain the same, both before and after the jump. The difference lies in the strength of the fundamental and higher order harmonics, cf. Figure 8 (b). This suggests that, although a global Volterra series representation is not possible from the description of the original system (1) for the range after the jump, a local Volterra series representation is still possible by means of discrete time parametric modelling.

First, the discrete time domain Volterra expression is introduced as

$$y(k) = \sum_{n=1}^{\infty} y_n(k) \tag{11}$$

where

$$y_n(k) = \sum_{-\infty}^{\infty} \cdots \sum_{-\infty}^{\infty} h_n(\tau_1, \cdots, \tau_n) \prod_{i=1}^{n} u(k - \tau_i) \qquad n > 0, k \in Z$$

A discrete time Volterra series is also called a NX (Nonlinear model with eXogenous inputs) model. Such an NX model can be built at the after-jumping point *A*=9.09, presented in (12). Here the excitation and response data were collected by stimulating the system (1) using 5th order Runge-Kutta method at a sampling interval $\pi/60$.

$$\begin{aligned} y(k) = 3.1948\, u(k-2) - 2.2584\, u(k-1) + 0.00882\, u^3(k-2) \\ - 0.00721\, u^2(t-1) u(t-2) \end{aligned} \qquad (12)$$

The relevant Model Predicted output, which shows a perfect match with the real response, is given in Figure 9. Apparently Figure 9 suggests that the Duffing oscillator (1) at the after-jumping point *A*=9.09 can be very accurately modelled by the Volterra series model (12) with only up to 3rd order kernels.

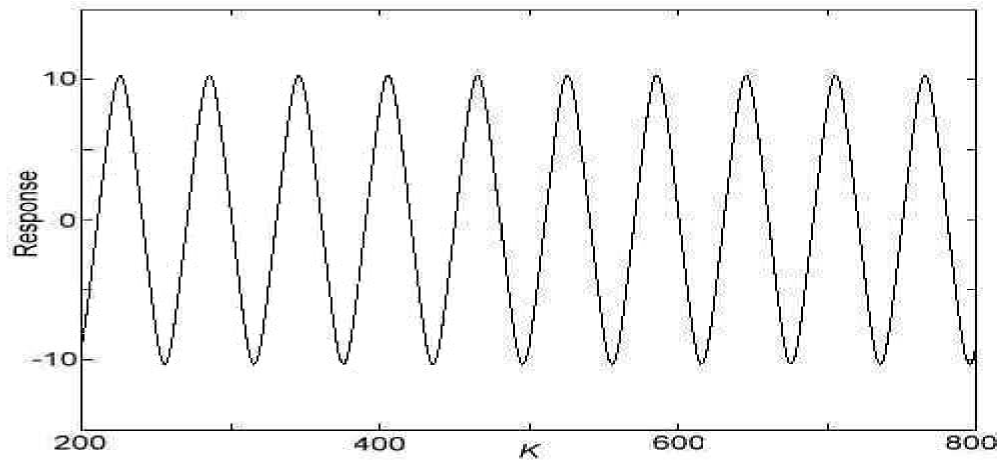

Figure 9. Model Predicted Output by NX model (12): MPO—dashed; Real response--solid

The NX model (12) can be mapped into the frequency domain to obtain $H_1(\cdot)$ and $H_3(\cdot)$ (Peyton Jones and Billings, 1989). For comparison, the first order frequency response function at the before-jumping and after-jumping points is listed in Table 1. A significant increase of $H_1(\omega)$ in magnitude is observed after the jump in order to compensate for the shock increase of the amplitude of response.

$\lvert H_1(\omega)\rvert$ from (8) at *A*=9.08	$\lvert H_1(\omega)\rvert$ from (12) at *A*=9.09
0.3304	0.9777

Table 1. $H_1(\omega)$ before and after the jump

The above analysis can be extended to a more general situation over a full range of excitation frequencies.

4. Volterra Modelling of the Duffing Equation with Varying Excitation Frequency

Consider system (1) with the coefficients in (8). This time the amplitude of the excitation is kept constant at *A*=1. On knowing the amplitude of excitation when the jump occurs, the new criterion (7) can also be used to determine the corresponding frequency where a jump is displayed. In the current example, this frequency is calculated from (7) as $\omega = 1.28$ rad/sec, which is a very good agreement with the simulation results of the resonance response curve in Figure 10.

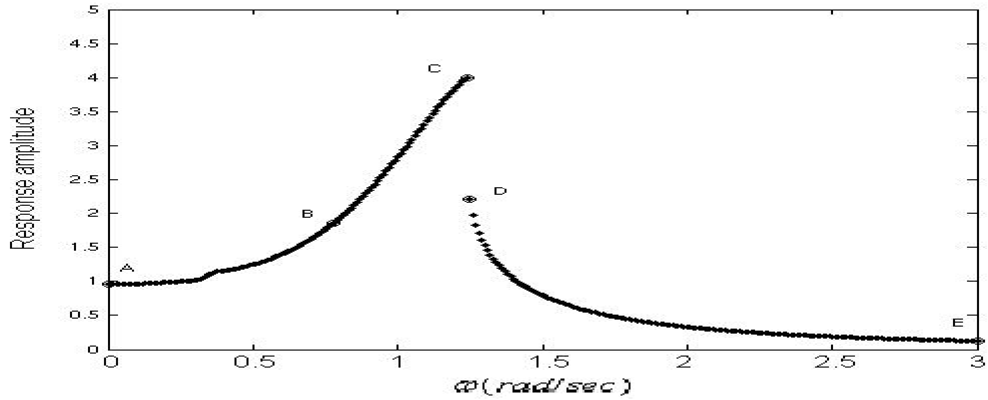

Figure 10. Resonance response curve for Duffing Equation (1) with *A*=1

Clearly there is a jump in the response from point C to point D, which suggests a severe behaviour change at this location. This will be studied by an inspection of (10) in the frequency domain using RSM in Figure 11.

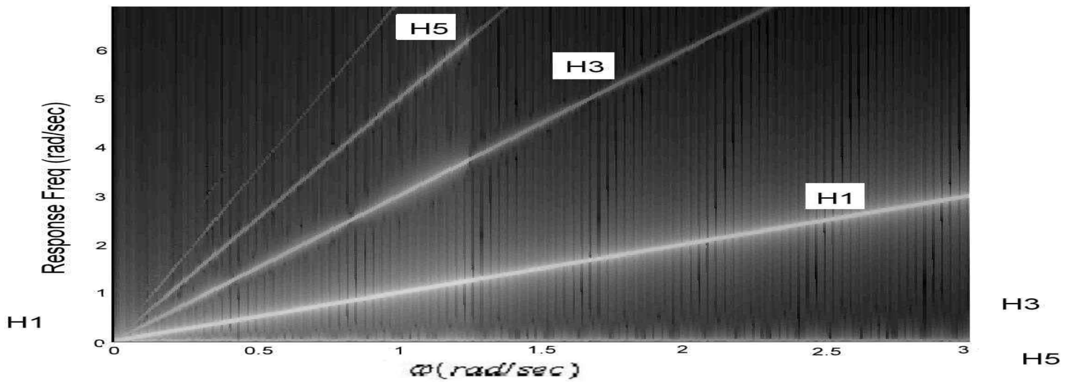

(a)

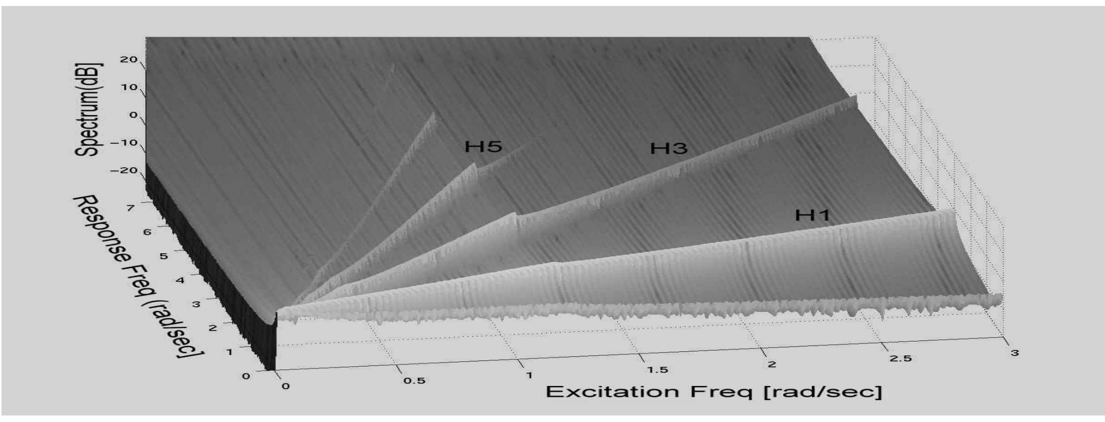

(b)

Figure 11. Response spectrum map for Duffing Equation (1) with *A*=1: (a) 2D view and (b) 3D view

It can be seen that as the frequency ω increases, the GFRF's derived from equation (8) are valid for the range A to B(ω=0.75rad/sec) in Figure 10. The GFRF's start to become invalid for the range B to C(ω=1.28) in Figure 10, and become valid again for the range D to E. In other words, in the frequency domain, besides the same jump point as in the time domain at ω=1.28, there is another change point at around ω=0.75. However, the change at around ω=0.75 develops gradually, and is not as abrupt as the 'jump' at ω=1.28. This kind of frequency domain change does not appear to be revealed by traditional tools, such as the resonance diagram in Figure 10. The Response Spectrum Map, which is plotted in Figure 11, does provide some information about this frequency domain change. First of all, there are no subharmonics shown in Figure 11, suggesting that the system for the whole frequency range of interest could be mildly nonlinear and that a valid Volterra/frequency domain representation could exist over all the frequency range. Secondly, the apparent 'jump' from C to D at frequency point ω=1.28 in Figure 10 is clearly detected by the change of magnitude in first order(linear) harmonic line H1 and the subsequent higher order harmonic lines H3, H5, etc with a weaker harmonic presence. The 3D plot Figure 11(b) further reveals that bigger drops are found in the higher order harmonic lines H3, H5 after the jump, with the H5 fade off very quickly. Since the higher order harmonics are associated with the higher order GFRF's, this means that before the jumping the potential Volterra series representation should have a more significant higher order kernel presence. Finally the frequency domain change at point B in Figure 10 is not detected on the dominant first order(linear) harmonics line H1, but again the H3 line shows a significant third order harmonic change around the frequency point ω=0.75. In order to find the frequency domain representation for the range B to C, the technique in section 3 can be used repeatedly, that is, discrete time Volterra-- or equivalently NX—models can be identified from each pair of single tone excitation and response data, over the frequency range [0.75, 1.28]. For example, for excitation frequency ω=1, the corresponding discrete time Volterra model can be expressed, with a sample frequency $f_s = 60/\pi$, as

$$\begin{aligned} y(k) &= 26.816\,u(k-2) - 24.40\,u(k-1) + 1.3984\,u^3(k-2) \\ &\quad - 1.3792\,u^2(k-1)u(k-2) \end{aligned} \tag{13}$$

from which the $H_1(\cdot)$ and $H_3(\cdot)$ data at frequency ω=1 can be obtained(Peyton Jones and Billings, 1989).

By repeating this procedure for a number of excitation frequencies along [0.75, 1.28], the GFRF's can be acquired by putting together the frequency response data recorded at each frequency point. The first order frequency response function $H_1(\cdot)$ computed in this manner is plotted in Figure 12 (dashed).

Using the approach introduced in Li and Billings(2001), a nonlinear continuous time model reconstructed from the $H_1(\cdot)$ and $H_3(\cdot)$ data, is given below

$$\begin{aligned} &y + 0.21727\tfrac{dy}{dt} + 0.87564\tfrac{d^2y}{dt^2} + 0.01713\tfrac{d^3y}{dt^3} + 0.18005\tfrac{d^4y}{dt^4} + 0.01939y^3 - 0.002162y^2\tfrac{dy}{dt} \\ &- 0.04358y(\tfrac{dy}{dt})^2 + 0.0001961(\tfrac{dy}{dt})^3 = u(t) \end{aligned} \tag{14}$$

The $H_1(\cdot)$ computed from equation (14) (solid)(Billings and Peyton Jones, 1990) is compared with the $H_1(\cdot)$ from the Volterra modelling such as equation (13), in Figure 12, which shows a good match.

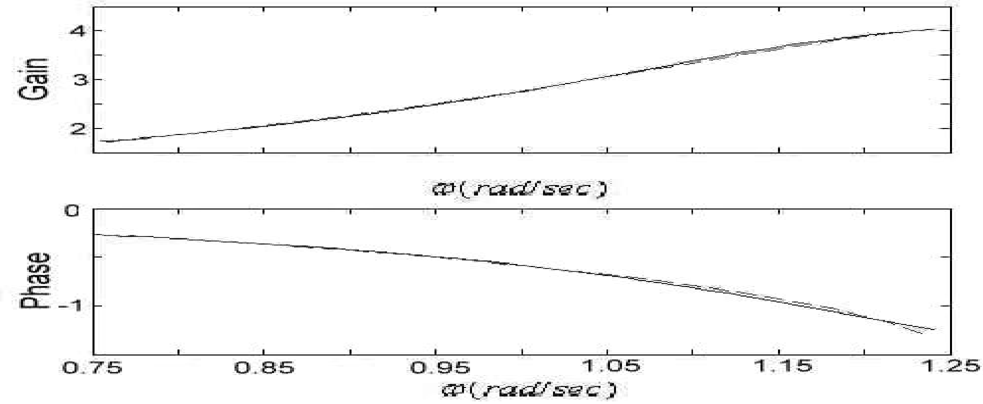

Figure 12. $H_1(\cdot)$ **by reconstructed continuous time model (14) –solid and** $H_1(\cdot)$ **by Volterra modellings—dashed**

To test the validity of the reconstructed continuous time model (14), arbitrarily choose an excitation frequency from the specific frequency range [0.75, 1.28], say, ω=0.9 rad/sec, and compare the response from the original Duffing equation (8) and the response synthesized from the GFRF's obtained from equation (14). It can be seen that up to third order GFRF's from (14) can provide a satisfactory representation for the system, as shown in Figure 13.

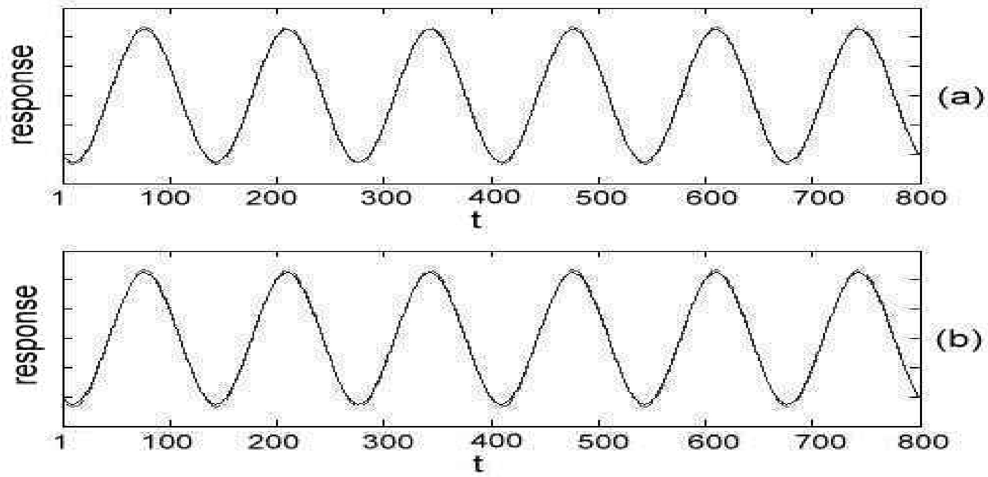

Figure 13 (a) First order output response, and (b) up to the third order response Solid— synthesized output by GFRF's from (14); Dashed--simulated original output from (8)

In summary the whole picture of the frequency domain representation for the Duffing oscillator (10) when the excitation amplitude is fixed as *A*= 1 would look like Figure 14 for the first order frequency response function for example. In summary, the frequency response function initially follows H_1 from the original Duffing equation (10) from A to B, then moves to H_1 by the new equation (14) from B to C, and finally jumps back to H_1 by the original Duffing equation (8) from D to E.

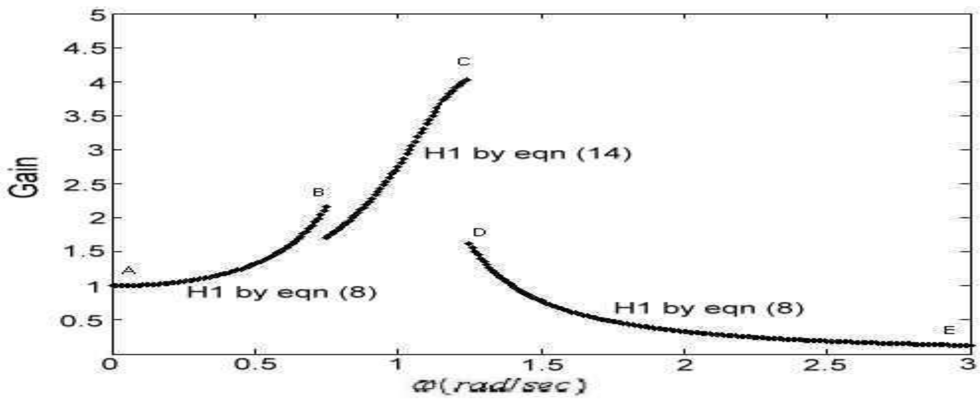

Figure 14. First order frequency domain response function for the Duffing oscillator (8)

5. Conclusions

The jump phenomenon is a common severe nonlinear dynamic behaviour found in many Duffing oscillators. The discussion in this paper shows that the jump is the dividing point between the validity of the Volterra series representation, or in other words, the absolute upper limit of a valid Volterra representation, therefore the new frequency domain criterion developed in the Part I of this paper can be readily used in predicting the onset point of the jump, which is proved to be very successful. The scheme behind the derivation of the new criterion, that is, the nonlinear system should be efficiently described by the first few Volterra kernels, can at the same time provide some explanation of the mechanism of the formation of the jump.

A global Volterra series representation for the nonlinear oscillator involving jump phenomenon is not expected due to the analytic nature of the Volterra description. However local Volterra series representations are still possible. This point has been discussed and analysed using illustrative examples in this study.

Acknowledgement: The authors gratefully acknowledge that this work was supported by the Engineering and Physical Sciences Research Council(EPSRC) UK, and a European Research Council Advanced Investigator Award.

References:

Billings, S.A. and Boaghe, O.M., 2001,The response spectrum map, a frequency domain equivalent to the bifurcation diagram, Int. J. of Bifurcation and Chaos, Vol.11, No.7, pp.1961-1975.

Billings, S.A. and Peyton Jones, J.C., 1990, Mapping non-linear integro-differential equations into the frequency domain, Int.J.Control, Vol. 52, No. 4,pp.863-879.

Boaghe, O.M. and Billings, S.A., 2003, Subharmonic Oscillation Modelling and MISO Volterra Series, IEEE Trans on Circuits And Systems—I: Fundamental Thoery And Applications, Vol. 50, No.7., pp877-884.

Feigenbaum, M.J., 1980, "Universal behaviour in nonlinear systems", Los Alamos Science, Vol.1, pp.4-27, in "Universality in chaos", Ed. Predrag Cvitanovic, pp.49-84, 1989.

Frey, D.R.and Norman, O., 1992, "An integral equation approach to the periodic steady-state problem in nonlinear circuits", IEEE Transactions on Circuits and Systems I - Fundamental Theory and Applications, Vol.39, No.9, pp.744-755.

Frey, D.R., 1998, "A class of relaxation algorithms for finding the periodic steady-state solution in nonlinear systems", IEEE Transactions on Circuits and Systems I - Fundamental Theory and Applications, Vol.45, No.6, pp.659-663.

Hayashi, C.,1964, Nonlinear oscillations in physical systems. , McGraw-Hill, New York.

Li, L.M. and Billings, S.A., 2001, Continuous time non-linear system identification in the frequency domain, Int J Control, 74 (10), pp. 1052-1061.

Li, L.M. and Billings, S.A., 2005, Discrete Time subharmonic modelling and Analysis, Int J Control， Vol. 78， No. 16, pp. 1265-1284.

Nayfeh, A.H. and Mook, D.T., 1979, "Nonlinear oscillations", John Wiley and Sons, New York.

Pain, H.J., 2005, The Physics of Vibrations and Waves, John Wiley & Sons, Ltd.

Peng, Z.K. and Lang,Z.Q., 2007,On the convergence of the Volterra-series representation of the Duffing's oscillators subjected to harmonic excitations, J. of Sound and Vibration, Vol. 305, pp.322-332.

Peyton Jones, J.C. and Billings, S.A., 1989, A Recursive algorithm for computing the frequency response of a class of non-linear difference equation models, Int.J.Control, Vol.50, No.5, pp.1925-1940.

Rao, S.S., 1995, "Mechanical vibrations", Addison-Wesley, New York.

Stoker, J.J., 1957, "Nonlinear vibrations in mechanical and electrical systems", Inter-science Publishers, Inc., New York.

Thompson, J.M.T. and Stewart, H.B., 1991, "Nonlinear dynamics and chaos", John Wiley and Sons, New York.

Tomlinson, G.R., Manson, G. and Lee, G.M., 1996, A simple criterion for establishing an upper limit to the harmonic excitation level of the Duffing oscillator using the Volterra Series, J. of Sound and Vibration, Vol. 190, No. 5, pp.751-762.